

Ballistic heat conduction and mass disorder in one dimension

Zhun-Yong Ong^{*} and Gang Zhang[†]

*Institute of High Performance Computing, A*STAR, Singapore 138632*

Abstract

It is well-known that in the disordered harmonic chain, heat conduction is subballistic and the thermal conductivity (κ) scales asymptotically as $\lim_{L \rightarrow \infty} \kappa \propto L^{0.5}$ where L is the chain length. However, using the nonequilibrium Green's function (NEGF) method and analytical modeling, we show that there exists a critical crossover length scale (L_C) below which ballistic heat conduction ($\kappa \propto L$) can coexist with mass disorder. This ballistic-to-subballistic heat conduction crossover is connected to the exponential attenuation of the phonon transmittance function Ξ *i.e.* $\Xi(\omega, L) = \exp[-L/\lambda(\omega)]$, where λ is the frequency-dependent attenuation length. The crossover length can be determined from the minimum attenuation length which depends on the maximum transmitted frequency. We numerically determine the dependence of the transmittance on frequency and mass composition as well as derive a closed form estimate which agrees closely with the numerical results. For the length-dependent thermal conductance, we also derive a closed form expression which agrees closely with numerical results and reproduces the ballistic to subballistic thermal conduction crossover. This allows us to characterize the crossover in terms of changes in the length, mass composition and temperature dependence, and also to determine the conditions under which heat conduction enters the ballistic regime. We describe how the mass composition can be modified to increase ballistic heat conduction

I. INTRODUCTION

It is commonly believed that in the absence of mass disorder, phonons propagate ballistically without dissipation in pristine one-dimensional (1D) harmonic systems, resulting in a linear relationship between the thermal conductivity κ and length L . [1] On the other hand, it is well-established from numerical and analytical results that the presence of mass disorder causes phonon localization [1–10], leading to a sublinear κ - L relationship ($\kappa \propto L^\alpha$ where $\alpha < 1$) in the asymptotic ($L \rightarrow \infty$) limit. This heat conduction scaling behavior is commonly termed subballistic or superdiffusive in the literature. [1, 5, 6] It also implies that the presence of mass disorder and localization [3, 11] is incompatible with ballistic heat conduction although its mere presence is not sufficient for the normal heat diffusion behavior. [1, 5, 6]

However, recent measurements of the thermal conductivity in micrometer-long SiGe-alloy nanowires at room temperature by Hsiao and co-workers have yielded a linear κ - L relationship,[12] suggesting the possibility of micrometer-scale ballistic phonon transport despite the presence of mass disorder. Thus, a fresh examination of the relationship between phonon localization and propagation in 1D systems is needed to understand this result *i.e.* the coexistence of ballistic heat conduction and mass disorder. This requires us to determine the conditions for ballistic conduction to occur in a disordered 1D structure. It also raises the question of how localization varies with the mass composition of the system and if there are any other experimentally detectable physical signatures, apart from the linear κ - L relationship, that can distinguish ballistic and subballistic heat conduction. This is important since the experimental determination of the κ - L relationship requires the fabrication and measurement of different samples of varying length,[13] and the process of fabricating samples of different sizes may introduce variability in the measured thermal conductivity. Such measurement variability between samples can obscure the signs of ballistic heat conduction. Therefore, it would be useful to be able to verify this phenomenon in a *single* sample.

To understand the coexistence of ballistic heat conduction and mass disorder, we revisit in this paper the phenomenon of phonon propagation in the disordered 1D harmonic lattice which we take to represent an idealization of real 1D systems with mass disorder.[9, 14, 15] Although this model may be simple, it is sufficient for our purpose of demonstrating and

clarifying the coexistence of ballistic heat conduction and mass disorder. Thus, it can be applied to elucidate the essential physics of phonon transport in quasi-1D systems with disorder as well as for the analysis and interpretation of experiments. [12, 16–18] Its simplicity also enables us to relate our numerical results to known analytical results from conventional wave transmission theory and to pinpoint the experimentally relevant physical parameters affecting phonon transmission in the presence of mass disorder. The purpose of our paper is to analyze the coexistence of ballistic heat conduction and mass disorder within the established framework of phonon localization. We show how ballistic heat conduction can occur in the presence of disorder and how it can be distinguished from subballistic heat conduction. Although the *asymptotic* scaling theory of heat conduction [2, 4, 14] and the localization phenomenon are rather well understood, the implications for *finite* systems have not been clarified. Neither has there been any attempt to use these disordered 1D models to relate the heat conduction phenomenon to experimentally relevant variables such as impurity concentration and temperature.

The organization of our paper is as follows. We first analyze how mass disorder affects phonon transmittance. While it is known that mass disorder attenuates phonon propagation and that the transmittance attenuation length (λ) scales as the inverse square frequency (ω^{-2}) for low-frequency modes in the $L \rightarrow \infty$ and $\omega \rightarrow 0$ limit, [2, 4] there is no straightforward numerical presentation of this result in the context of heat conduction. We use the standard nonequilibrium Green’s function (NEGF) method to compute the frequency-dependent transmittance for chain of different lengths with different values of impurity mass. We compare the transmittance with known analytical estimates and find a reasonably good fit over a wide range of frequencies, allowing us to find the dependence on mass composition. A close analogy to the Beer-Lambert law is also found. This enables us to find a good closed form estimate of the thermal conductance, from which we are able to deduce its dependence on mass composition. We also derive from the closed form expression the dependence of the thermal conductance on length, mass composition and temperature. More importantly, we show and summarize how these dependences differ in the ballistic and subballistic regime. Given that large lattices are expected to exhibit a sublinear κ - L relationship in the $L \rightarrow \infty$ limit, we identify the crossover length scale (L_C) below which phonon transport acquires a fully ballistic character independent of mass composition and above which phonon transport is affected by lattice disorder. We also show how the crossover length can be tuned by

changing the impurity concentration and mass difference.

II. SIMULATION METHODOLOGY

We choose as our model system the familiar 1D harmonic lattice first studied by Dyson. [19] Our system differs from that used in other papers in that the atomic mass is not treated as a continuous random variable. Rather, we have a random binary lattice (RBL), where the positions of the component atoms are randomly shuffled, which resembles more realistic systems with mass disorder and allows us to quantify the effect of experimentally relevant variables such as impurity concentration and mass difference on thermal conduction. For simplicity, only adjacent atoms are coupled. We do not expect our results to be qualitatively different with longer-range interactions since the interaction typically grows weaker with interatomic distance. The atoms are only permitted to move longitudinally and no attempt is made to include any anharmonic interaction in our model.

Our system consists of three parts. In the middle, there is a finite-size ‘conductor’ of N equally spaced atoms. On either side, there is a homogeneous lead *i.e.* a semi-infinite chain with no mass disorder. In effect, we have a finite disordered system embedded in an *infinite* homogeneous 1D lattice. Coupling between adjacent atoms is governed by the harmonic spring term $V(x_i, x_{i+1}) = \frac{1}{2}k(x_i - x_{i+1})^2$ where k is the spring constant and x_i is the displacement of the i -th atom from its equilibrium position. In the RBL, there are two species of atoms which we label ‘A’ and ‘B’. Species ‘A’ is taken to be the substitutional impurity and exists only within the conductor. The rest of the atoms in the conductor and the leads are of species ‘B’. We set the mass of the B atoms to $m_B = 4.6 \times 10^{-26}$ kg (the mass of a Si atom), the spring constant to $k = 32$ Nm⁻¹ (the approximate strength of the Si-Si bond) and the interatomic spacing to $a = 0.55$ nm. Our choice of parameters follows that in Ref. [20]. We vary the ratio of the masses ($R = \frac{m_A}{m_B}$) and concentration ($c_A =$ fraction of A atoms, $c_B = 1 - c_A$) in our simulations. The 1D lattice size is varied from $N = 100$ to 20000, and the equivalent range of chain length values ($L = Na$) is $L = 55$ nm to 1.1 μ m. A schematic of the system is shown in Fig. 1.

To simulate phonon transport, we use the nonequilibrium Green’s function (NEGF) method which is described in detail in Refs. [20, 21]. The method calculates the frequency-dependent energy transmittance function $\Xi(\omega)$ by modeling the conductor as an open quan-

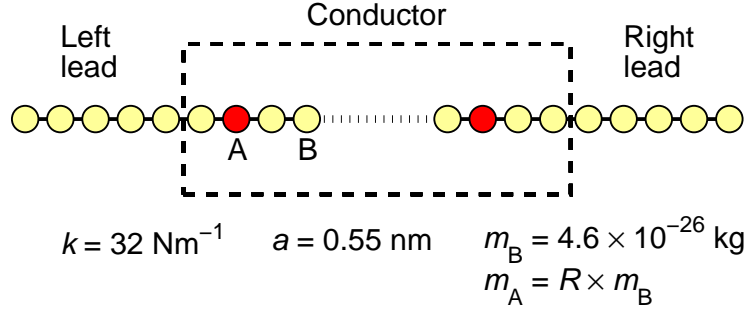


Figure 1: Schematic of the 1D random binary lattice. The atomic parameters are taken from Ref. [20].

tum system and the semi-infinite leads as self-energies (open boundaries). The Green's function for the conductor is

$$\mathbf{G}(\omega) = [\omega^2 + i0^+ - \mathbf{K}_C - \mathbf{\Sigma}_L(\omega) - \mathbf{\Sigma}_R(\omega)]^{-1},$$

where $\mathbf{\Sigma}_L$ ($\mathbf{\Sigma}_R$) is the so-called self-energy corresponding to the left (right) semi-infinite lead; \mathbf{K}_C is the force constant matrix of the conductor, and its (i, j) matrix element which couples the i -th and j -th atom is given by

$$[\mathbf{K}_C]_{ij} = (m_i m_j)^{-1/2} \frac{\partial^2 V}{\partial x_i \partial x_j}.$$

To compute $\Xi(\omega)$, we use the Caroli transmission formula [22] $\Xi(\omega) = \text{Tr}(\mathbf{\Gamma}_L \mathbf{G} \mathbf{\Gamma}_R \mathbf{G}^\dagger)$, where $\mathbf{\Gamma}_L$ ($\mathbf{\Gamma}_R$) is the term coupling the conductor to left (right) lead. [20, 21] As with any study of disordered systems, it is necessary to express the computed variables in terms of their ensemble average. In this paper, the ensemble-average transmittance function $\langle \Xi(\omega) \rangle$ is obtained by averaging $\Xi(\omega)$ over 100 realizations of the RBL.

It is more useful to work with the thermal conductance σ which is related to the thermal conductivity via the relation $\kappa \propto \sigma L$. The thermal conductance is computed using the Landauer formula: [20, 21]

$$\sigma(T) = \frac{1}{2\pi} \int_0^\infty \hbar \omega \frac{df(\omega)}{dT} \langle \Xi(\omega) \rangle d\omega \quad (1)$$

where T and \hbar are respectively the temperature and reduced Planck constant, and $f(\omega) = [\exp(\frac{\hbar \omega}{k_B T}) - 1]^{-1}$ is the Bose-Einstein occupation factor. The expression in Eq. (1) integrates the frequency-dependent transmittance spectrum and the differential heat capacity over the

entire frequency range (0 to ∞). In the high temperature limit, we have $f(\omega) \approx \frac{k_B T}{\hbar \omega}$ so that Eq. (1) becomes:

$$\lim_{T \rightarrow \infty} \sigma(T) = \frac{k_B}{2\pi} \int_0^\infty \langle \Xi(\omega) \rangle d\omega , \quad (2)$$

which is proportional to the *total* transmittance. In the case of the homogeneous chain ($m_A = m_B$), the transmittance is $\Xi(\omega) = \Theta(\omega_C - \omega)$ where $\omega_C = 2\sqrt{k/m_B}$ is the frequency cutoff, and Eq. (2) yields a length-independent thermal conductance *i.e.* $\lim_{T \rightarrow \infty} \sigma(T) = \frac{k_B \omega_C}{2\pi}$. This example implies that a length-dependent transmittance function is needed for the conductance to vary with L .

III. RESULTS AND DISCUSSION

A. Length dependence of transmittance spectrum

Given that the transmittance spectrum is expected to vary with L , the question arises as to what its dependence on L should be. In general, the transmittance function can be interpreted as the ease with which a phonon traverses the conductor. To identify the functional relationship, we first compute $\langle \Xi(\omega) \rangle$ for different values of chain length L at different values of R and c_A . Figure 2 shows $\langle \Xi(\omega) \rangle$ decreasing with increasing ω and L for a particular combination of c_A and R ($c_A = 0.5$ and $R = 2$), with the rate of decrease faster for higher-frequency modes. From our calculations, we find that $\langle \Xi(\omega, L) \rangle$ obeys the simple numerical relation:

$$\langle \Xi(\omega, L) \rangle = \langle \Xi(\omega, L_0) \rangle \exp \left[-\frac{L - L_0}{\lambda(\omega)} \right] , \quad (3)$$

for $\omega < \omega_C$ and $L > L_0$, analogous to the *Beer-Lambert* law in optics. The parameter $\lambda(\omega)$ is the frequency-dependent attenuation length and can be interpreted as the distance through which the phonon has its transmitted square amplitude reduced by a factor of $1/e$. Numerical fitting yields the numerical relationship $\lambda \propto \omega^{-2}$.

To determine the exact relationship between λ and ω , we use the recent result from Das and Dhar, [23] who proved an intuitive and useful formula relating the energy transmittance $\Xi(\omega)$ and the plane-wave transmission function $\tau(\omega)$ for the 1D harmonic chain:

$$\Xi(\omega) = |\tau(\omega)|^2 . \quad (4)$$

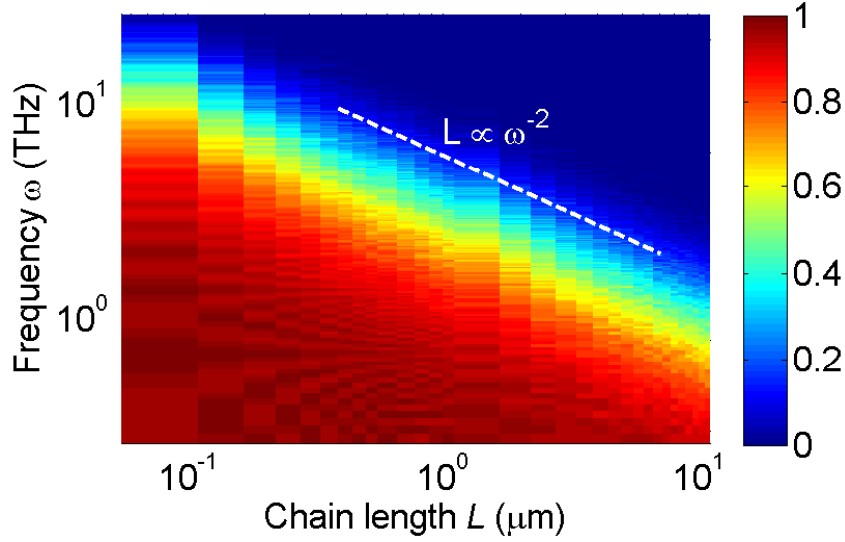


Figure 2: Two-dimensional plot of the transmittance function $\langle \Xi(\omega, L) \rangle$ as a function of frequency ω and chain length L for $c_A = 0.5$ and $R = 2$. The plot shows that the transmittance decreases as the chain length increases. The transmittance of the low-frequency modes is relatively unattenuated by the increase in L while the transmittance of the higher-frequency modes ($\omega \gtrsim 1$ THz) decays rapidly with increasing L . The position of the ‘shoulder’ (ω), corresponding to the cyan region and $\langle \Xi \rangle \sim 1/e$, shifts towards the origin as L increases and varies as $L \propto \omega^{-2}$ (line is drawn in white).

In the disordered harmonic chain with N atoms, the ensemble average of its asymptotic amplitude has the form of an exponentially decaying function *i.e.* $\lim_{N \rightarrow \infty} |\tau(\omega)| = \exp[-\gamma(\omega)N]$ where γ is the dimensionless Lyapunov exponent. [2, 4] This implies that the attenuation length in Eq. (3) is

$$\lim_{L \rightarrow \infty} \lambda(\omega) = \frac{a}{2\gamma(\omega)}. \quad (5)$$

In the low frequency ($\omega \rightarrow 0^+$) limit, the closed form expression for γ is known [2] and given by

$$\lim_{\omega \rightarrow 0} \gamma(\omega) = \frac{\langle \delta m \rangle^2 \omega^2}{8k\langle m \rangle}, \quad (6)$$

where $\langle \delta m \rangle$ and $\langle m \rangle$ are respectively the standard deviation and the mean of the conductor atomic mass. Combining Eqs. (6) and (5), we obtain the expression for the low-frequency attenuation length

$$\lambda_0(\omega) = \frac{4ka\langle m \rangle}{\langle \delta m \rangle^2 \omega^2} \quad (7)$$

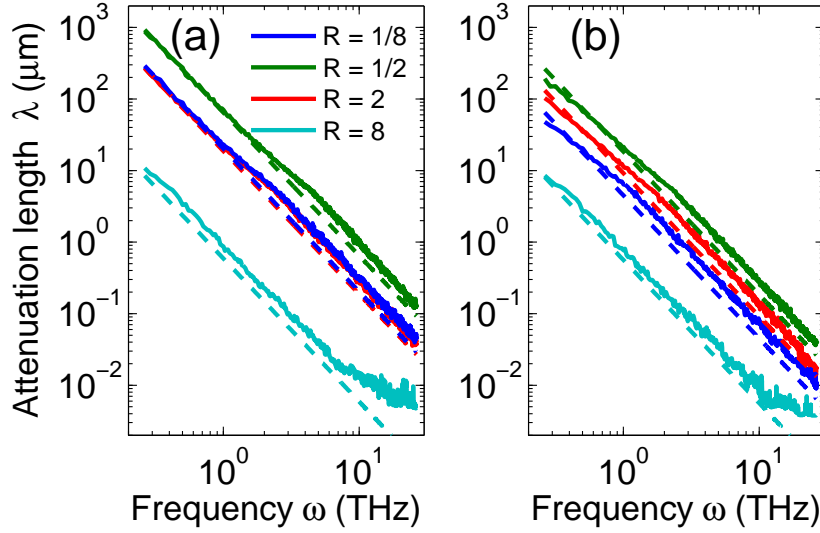


Figure 3: Plot of the extracted attenuation length λ (solid lines) and its low-frequency estimate λ_0 (dashed lines) as a function of ω for $R = 1/8, 1/2, 2$ and 8 at (a) $c_A = 0.1$ and (b) $c_A = 0.5$. At low frequency ($\omega < 1$ THz), there is very good agreement between λ_0 and λ , as expected. At higher frequencies, λ is slightly larger than λ_0 . The approximation λ_0 however diverges increasingly from the extracted attenuation length λ as λ_0 approaches a , the interatomic spacing.

which we plot in Fig. 3 together with $\lambda(\omega)$ for $R = 1/8, 1/2, 2$ and 8 at $c_A = 0.1$ and 0.5 . We find close agreement between the two at low frequencies ($\omega < 1$ THz). At higher frequencies, $\lambda_0(\omega)$ is slightly smaller but still an excellent approximation to the numerically computed $\lambda(\omega)$. The approximation λ_0 however diverges increasingly from the extracted attenuation length λ as λ_0 approaches a , the interatomic spacing. This is more evident for the $R = 8$ curve in Fig. 3 when the impurity mass m_A is much greater than m_B .

If we interpret $\lambda_0(\omega)$ as an impurity-limited mean free path (MFP) and assume a very dilute impurity concentration $n_{\text{imp}} = c_A \ll 1$, then we have $\langle \delta m \rangle^2 = c_A(1 - c_A)(m_A - m_B)^2 \approx n_{\text{imp}}(m_A - m_B)^2$ and obtain $\lambda_0 \propto n_{\text{imp}}^{-1}(m_A - m_B)^{-2}\omega^{-2}$ *i.e.* the attenuation length varies as n_{imp}^{-1} . This parallels the Beer-Lambert law for photons where the attenuation length is inversely proportional to the absorber concentration. In three dimensions, the impurity-limited MFP [$\lambda_{\text{imp,3D}} \propto n_{\text{imp}}^{-1}(m_A - m_B)^{-2}\omega^{-4}$] has identical dependence on impurity concentration and mass difference but a very different frequency dependence. [24]

B. Length, mass composition and temperature dependence for ballistic and sub-ballistic thermal conductance

Having numerically verified the form of the transmittance function, we proceed to calculate the thermal conductance to determine its dependence on length, mass composition and temperature. From Eqs. (1), (6) and (5), we arrive at an analytical expression for estimating the length-dependent thermal conductance:

$$\sigma_0(T, L) = \frac{1}{2\pi} \int_0^{\omega_C} \hbar\omega \frac{df}{dT} \exp \left[-\frac{L\langle\delta m\rangle^2\omega^2}{4ka\langle m\rangle} \right] d\omega . \quad (8)$$

This approximation relies on the $\lim_{L \rightarrow \infty, \omega \rightarrow 0^+} \lambda(\omega)$ expression in Eq. (5) *i.e.* it makes use of the *low-frequency* approximation for $\lambda(\omega)$ in the $L \rightarrow \infty$ limit. At finite L , higher-frequency modes contribute more to the phonon transmittance and their attenuation behavior may not follow that of Eq. (6).

To see how well Eq. (8) approximates the thermal conductance σ (calculated from NEGF) especially for *finite* L , we compute σ_0 for $R = 2$ and $c_A = 0.1$ at $T = 300$ K and plot it in Fig. 4 together with the corresponding σ . σ_0 scales as $L^{-0.5}$ and agrees well with σ but is consistently ~ 20 percent smaller. We have also computed σ_0 for other values of R and c_A and found that it is also ~ 20 percent smaller than σ computed from NEGF. This small discrepancy is expected given that Eq. (8) uses the low-frequency approximation λ_0 which overestimates the transmittance attenuation.

Since Fig. (4) shows that the expression for σ_0 from Eq. (8) can fit the numerically computed σ , it means that we can use Eq. (8) to infer the asymptotic behavior of the conductance in the $L \rightarrow \infty$ and $L \rightarrow 0$ limits. In the $L \rightarrow \infty$ limit, only very low frequency modes contribute to the integral in Eq. (8), allowing us to use the high-temperature approximation *i.e.*

$$\frac{df}{dT} = \frac{k_B}{\hbar\omega} ,$$

so that Eq. (8) becomes

$$\lim_{L \rightarrow \infty} \sigma_0(T, L) \approx \frac{k_B}{2\pi} \int_0^\infty \exp \left[-\frac{L\langle\delta m\rangle^2\omega^2}{4ka\langle m\rangle} \right] d\omega .$$

This yields

$$\lim_{L \rightarrow \infty} \sigma_0 = \left[\frac{ka\langle m\rangle k_B^2}{4\pi\langle\delta m\rangle^2} \right]^{\frac{1}{2}} \frac{1}{\sqrt{L}} \quad (9)$$

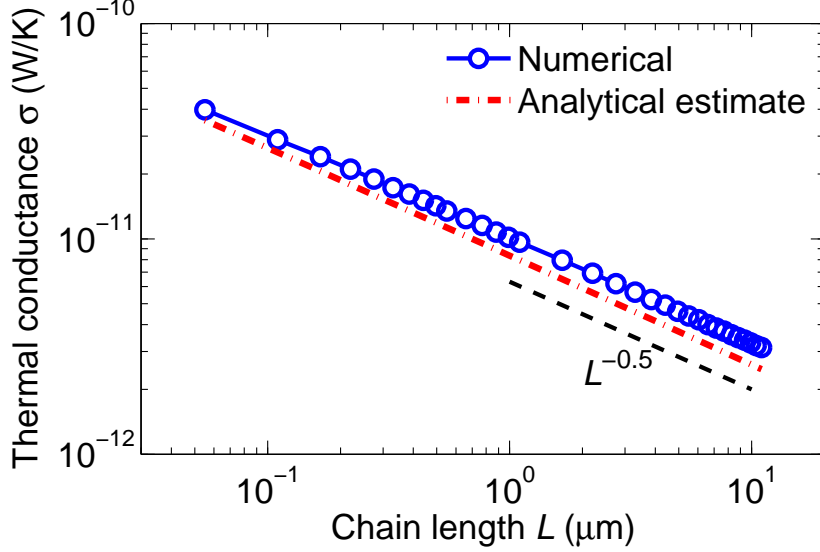


Figure 4: Plot of the length-dependent thermal conductances σ (circle) and σ_0 (dash-dot) computed respectively from the NEGF method and Eq. (8) for $R = 2$ and $c_A = 0.1$ at $T = 300$ K. σ_0 scales as $L^{-0.5}$ but is about 20 percent smaller than σ .

which gives the well-known $\lim_{L \rightarrow \infty} \sigma \propto L^{-0.5}$ relationship, [2, 4, 9] indicating subballistic (superdiffusive) thermal transport. In the $L \rightarrow 0$ limit, the conductor is transparent to all phonon modes with frequency below ω_C (the cutoff frequency determined by the atomic mass in the leads, m_B), *i.e.* $\Xi(\omega) \approx \Theta(\omega_C - \omega)$, and we recover the expression for the finite length-independent thermal conductance,

$$\lim_{L \rightarrow 0} \sigma_0 = \frac{1}{2\pi} \int_0^{\omega_C} \hbar \omega \frac{df}{dT} d\omega \quad (10)$$

which is *independent* of the mass composition. We note that the ballistic conductance in Eq. (10) is proportional to the heat capacity of the system.

Although the model described by Eq. (8) is very simple, the variation in its thermal transport character in the different limits, as suggested by Eqs. (9) and (10), has significant qualitative implications for more realistic experimental systems, apart from its $\sigma \propto L^{-0.5}$ property. We use them to deduce the difference in the dependence on the various physical variables. Firstly, in the *ballistic* limit, the thermal conductance is *independent* of its mass composition. On the other hand, in the *subballistic* limit, the conductance is inversely proportional to the standard deviation of the mass concentration, and in the *dilute* limit ($c_A \rightarrow 0$), it should scale as $\sigma \propto n_{\text{imp}}^{-0.5} |\Delta m|^{-1}$, where $\Delta m = m_A - m_B$ is the mass difference,

Physical variable	Scaling exponent α	
	Ballistic	Subballistic
	$(L \ll L_C)$	$(L \gg L_C)$
Length ($\sigma \propto L^\alpha$)	0	-0.5 to -0.4
Temperature ($\sigma \propto T^\alpha$)	1	0
Mass difference ($\sigma \propto \Delta m ^\alpha$)	0	-1
Impurity concentration ($\sigma \propto n_{\text{imp}}^\alpha$)	0	-0.5

Table I: Scaling dependence of the thermal conductance σ on various physical variables (length, temperature, mass difference and impurity concentration) in the ballistic ($L \ll L_C$) and subballistic ($L \gg L_C$) regime in the 1D random binary lattice.

since $\langle \delta m \rangle^2 = c_A c_B (m_A - m_B)^2 \approx n_{\text{imp}} \Delta m^2$ in Eq. (9). Secondly, the temperature dependence of the conductance is different for the subballistic and ballistic case. In the subballistic case ($L \rightarrow \infty$), the range of conducting phonon modes decreases as $L^{-0.5}$ and only the low-frequency modes contribute to thermal transport. Hence, the temperature dependence of the thermal conductance is negligible. However, in the ballistic case ($L \rightarrow 0$), the range of conducting modes ($\omega < \omega_C$) is determined by the phonon occupation in the leads. Thus, the conductance is more sensitive to temperature change and in the low-temperature limit ($T \ll \hbar \omega_C / k_B$), we obtain $\sigma_0 \propto T$. We summarize the differences in the scaling dependence of the thermal conductance in Table I. These differences can be used to distinguish the ballistic and subballistic transport regimes.

C. Ballistic to subballistic crossover length

Given that thermal conduction is ballistic in the $L \rightarrow 0$ limit and subballistic in the $L \rightarrow \infty$ limit, there must exist an intermediate length scale that marks the crossover from ballistic to subballistic thermal transport although we do not observe one in Fig. 4. Since the thermal conductance depends on the mass composition in the $L \rightarrow \infty$ limit [Eq. (9)], it implies that the crossover length varies with mass composition. This can be increased by weakening the amount of mass disorder so that ballistic heat conduction is detectable in the range of L values simulated.

For a dilute impurity concentration and small mass difference, the mass variance ($\langle\delta m\rangle^2$) is small and the mass disorder is weak. Thus, the crossover length between ballistic and subballistic thermal transport can be large. The crossover length scale L_C can be estimated by estimating the minimum possible attenuation length which is determined by the cutoff frequency ω_C . Using Eq. (7), we set $L_C = \lambda_0(\omega_C)$ which yields $L_C = a\langle m\rangle m_B/[c_A(1 - c_A)\Delta m^2]$. This suggests that the ballistic regime can be extended by reducing the impurity concentration as well as mass ratio (R). Instead of using $R = 2$, we pick a small R so that the mass difference would be small ($\Delta m \ll m_B$). Figure 5 shows the NEGF-computed σ and σ_0 from Eq. (8) as a function of L (56 nm to 88 μ m) for (R, C_A) equal to (1.05, 0.1), (1.05, 0.5), (1.1, 0.1), (1.1, 0.5), (1.2, 0.1) and (1.2, 0.5) in the high temperature ($T \rightarrow \infty$) limit. We find good agreement between σ and σ_0 over the range of L considered, with the agreement better for larger c_A and Δm . The corresponding crossover length ranges between $L_C \approx 0.05$ to 2 μ m. Below $L < L_C$, σ and σ_0 converge to the ballistic limit $\sigma = \frac{k_B\omega_C}{2\pi}$ while for $L \gg L_C$, $\sigma \propto L^{-\alpha}$ with $\alpha < 0.5$ and $\sigma_0 \propto L^{-0.5}$, respectively. The discrepancy in the length dependence between σ and σ_0 may be a consequence of the small mass variance. In the $\langle\delta m\rangle \rightarrow 0$ limit, we expect fully ballistic thermal transport *i.e.* $\sigma \propto L^0$. Thus, the scaling exponent would deviate from -0.5 toward 0 for small $\langle\delta m\rangle$.

IV. SUMMARY

In summary, we have studied heat conduction in the 1D random binary lattice model with mass disorder. We have shown that the energy transmittance attenuates exponentially with lattice size, similar to the Beer-Lambert law for photons. The attenuation length is shown numerically to have frequency dependence of $\lambda \propto \omega^{-2}$ for low frequency modes (as predicted by localization theory) and also for high frequency modes (not predicted by localization theory). The existence of a maximum cutoff frequency implies a minimum attenuation length below which the transmittance of the phonons in the system converges to unity. This indicates that ballistic heat conduction can coexist with mass disorder for finite systems. The crossover length between ballistic and subballistic heat conduction can be estimated based on the cutoff frequency ω_c and the low-frequency expression for the attenuation length λ_0 . This analytical estimate has been shown to agree closely with the numerical crossover length computed with NEGF. We have also derived the explicit length,

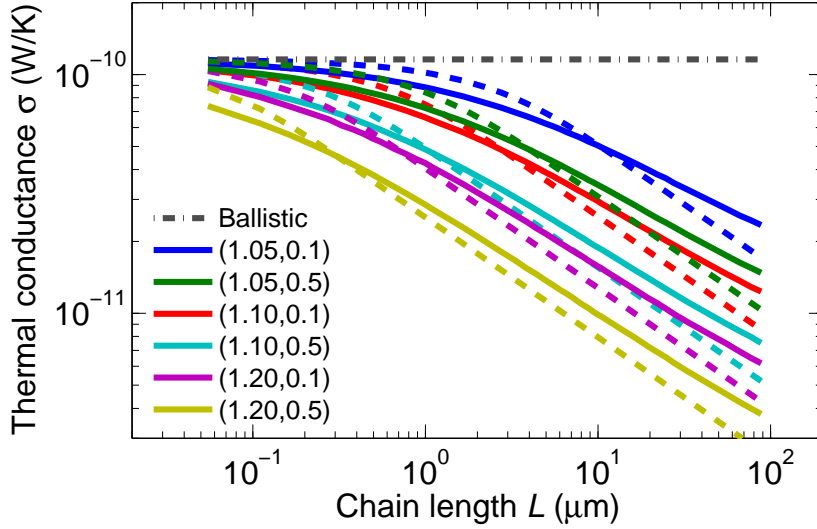


Figure 5: Plot of the NEGF-computed σ (solid line) and σ_0 from Eq. (8) (dashed line) for (R, c_A) equal to $(1.05, 0.1)$, $(1.05, 0.5)$, $(1.1, 0.1)$, $(1.1, 0.5)$, $(1.2, 0.1)$ and $(1.2, 0.5)$ in the high temperature ($T \rightarrow \infty$) limit in blue, green, red, cyan, magenta and yellow, respectively. The dash-dotted line shows the ballistic conductance in the homogeneous chain. There is good agreement between σ and σ_0 , with the fit improving as R increases. The ballistic-to-subballistic crossover is around L_C , ranging between 0.05 to 2 μm .

temperature and mass composition dependence of the thermal conductance and shown how they differ in the ballistic and subballistic limit. The differences can be used to distinguish ballistic and subballistic heat conduction in experimental systems. By making use of the mass composition dependence of the attenuation length, we have shown how the crossover between ballistic and subballistic heat conduction can be manipulated by changing the impurity mass difference and concentration.

The authors gratefully acknowledge the financial support from the Agency for Science, Technology and Research (A*STAR), Singapore and the use of computing resources at the A*STAR Computational Resource Centre, Singapore.

* Electronic address: ongzy@ihpc.a-star.edu.sg

† Electronic address: zhangg@ihpc.a-star.edu.sg

- [1] S. Lepri, R. Livi, and A. Politi, *Physics Reports* **377**, 1 (2003).
- [2] H. Matsuda and K. Ishii, *Suppl. Prog. Theor. Phys.* **45**, 56 (1970).
- [3] K. Ishii, *Suppl. Prog. Theor. Phys.* **53**, 77 (1973).
- [4] A. Dhar, *Phys. Rev. Lett.* **86**, 5882 (2001).
- [5] B. Li, H. Zhao, and B. Hu, *Phys. Rev. Lett.* **86**, 63 (2001).
- [6] B. Li and J. Wang, *Phys. Rev. Lett.* **91**, 044301 (2003).
- [7] J. M. Deutsch and O. Narayan, *Phys. Rev. E* **68**, 041203 (2003).
- [8] A. Kundu, *Phys. Rev. E* **82**, 031131 (2010).
- [9] X. Ni, M. L. Leek, J.-S. Wang, Y. P. Feng, and B. Li, *Phys. Rev. B* **83**, 045408 (2011).
- [10] J. D. Bodyfelt, M. C. Zheng, R. Fleischmann, and T. Kottos, *Phys. Rev. E* **87**, 020101 (2013).
- [11] P. W. Anderson, *Phys. Rev.* **109**, 1492 (1958).
- [12] T.-K. Hsiao, H.-K. Chang, S.-C. Liou, M.-W. Chu, S.-C. Lee, and C.-W. Chang, *Nat. Nanotech.* **8**, 534 (2013).
- [13] C. W. Chang, D. Okawa, H. Garcia, A. Majumdar, and A. Zettl, *Phys. Rev. Lett.* **101**, 075903 (2008).
- [14] I. Savić, N. Mingo, and D. A. Stewart, *Phys. Rev. Lett.* **101**, 165502 (2008).
- [15] T. Yamamoto, K. Sasaoka, and S. Watanabe, *Phys. Rev. Lett.* **106**, 215503 (2011).
- [16] P. Kim, L. Shi, A. Majumdar, and P. L. McEuen, *Phys. Rev. Lett.* **87**, 215502 (2001).
- [17] M. Fujii, X. Zhang, H. Xie, H. Ago, K. Takahashi, T. Ikuta, H. Abe, and T. Shimizu, *Phys. Rev. Lett.* **95**, 065502 (2005).
- [18] I.-K. Hsu, R. Kumar, A. Bushmaker, S. B. Cronin, M. T. Pettes, L. Shi, T. Brintlinger, M. S. Fuhrer, and J. Cumings, *Applied Physics Letters* **92**, 063119 (2008).
- [19] F. J. Dyson, *Phys. Rev.* **92**, 1331 (1953).
- [20] W. Zhang, T. Fisher, and N. Mingo, *Numerical Heat Transfer, Part B: Fundamentals* **51**, 333 (2007).
- [21] N. Mingo, in *Thermal Nanosystems and Nanomaterials* (Springer, 2009) pp. 63–94.
- [22] C. Caroli, R. Combescot, P. Nozieres, and D. Saint-James, *J. Phys. C* **4**, 916 (1971).
- [23] S. G. Das and A. Dhar, *Eur. Phys. J. B* **11**, 1857 (2012).
- [24] M. G. Holland, *Phys. Rev.* **132**, 2461 (1963).